# *Earthquake potential and ground shaking hazard at the Los Alamos National Laboratory*

Ivan G. Wong, Keith Kelson, Susan Olig, Jacqueline Bott, Robert Green, Thomas Kolbe, Mark Hemphill-Haley, Jamie N. Gardner, Steven Reneau, and Walter. Silva

1996, pp. 135-142. https://doi.org/10.56577/FFC-47.135

*in:*

*Jemez Mountains Region*, Goff, F.; Kues, B. S.; Rogers, M. A.; McFadden, L. S.; Gardner, J. N.; [eds.], New Mexico Geological Society 47th Annual Fall Field Conference Guidebook, 484 p. https://doi.org/10.56577/FFC-47

*This page is intentionally left blank to maintain order of facing pages.*

# EARTHQUAKE POTENTIAL AND GROUND SHAKING HAZARD AT THE LOS ALAMOS NATIONAL LABORATORY, NEW MEXICO

IVAN WONG[1], KEITH KELSON[2], SUSAN OLIG[1], JACQUELINE BOTT[1], ROBERT GREEN[1], THOMAS KOLBE[1], MARK HEMPHILL-HALEY[1], JAMIE GARDNER[3], STEVEN RENEAU[3] and WALTER SILVA[4]

[1]Woodward-Clyde Federal Services, 500 12th St., Suite 100, Oakland, CA 94607; [2]William Lettis & Associates, Inc. 1777 Botelho Dr., Walnut Creek, CA 94596; [3]Los Alamos National Laboratory, Los Alamos, NM 87545; [4]Pacific Engineering & Analysis, 311 Pomona Ave., El Cerrito, CA 94530

**Abstract**—A four-year program of geologic, seismologic, geophysical and geotechnical investigations recently evaluated the potential seismic hazards at the Los Alamos National Laboratory (LANL). In this study, 25 faults and four seismic source zones were identified as seismic sources potentially significant to LANL in terms of strong ground shaking. The source zones, such as the Rio Grande rift, in which the Laboratory is located, account for the hazard from "background" earthquakes that do not repeatedly rupture the surface and cannot be associated with known faults or tectonic features. All seismic sources were characterized in terms of their location, geometry, maximum magnitude and earthquake recurrence. The three most significant and closest faults to LANL (Pajarito, Guaje Mountain and Rendija Canyon faults, which comprise the Pajarito fault system) were the focus of detailed paleoseismic studies. The main 41-km-long Pajarito fault is located along the western margin of LANL and is a down-to-the-east normal fault, dipping beneath the Laboratory. The size of the maximum earthquake for the Pajarito fault is estimated to be moment magnitude ($M_w$) 6.9 ± 0.3 based on empirical relationships for rupture length, rupture area and displacement. The average long-term slip rate for the fault is about 0.1 mm/yr. The subsurface geology beneath LANL was characterized through a program of borehole exploration and velocity measurements, dynamic laboratory testing of borehole samples, and compilation and evaluation of all relevant borehole and geotechnical data. Site-specific geologic and velocity profiles for several LANL facility sites were developed based on these data. These geologic data and the seismic source characterization were input into a probabilistic seismic hazard analysis performed using a logic tree approach. Peak horizontal accelerations estimated for LANL are approximately 0.15, 0.30 and 0.56 g for the return periods of 500, 2000, and 10,000 years, respectively. The dominant seismic source contributing to the hazard at LANL is the Pajarito fault system and, to a lesser extent, the background earthquakes within the Rio Grande rift source zone.

## INTRODUCTION

The Los Alamos National Laboratory, a major U.S. Department of Energy (DOE) research facility operated by the University of California, is located within the Rio Grande rift, a tectonically, volcanically and seismically active seismotectonic province in the western United States. Although active on the microearthquake level, only six earthquakes of estimated Richter magnitude ($M_L$) 5.0 or greater have occurred in the LANL region (defined in Fig. 1) since 1873 (Sanford et al., 1991). The most significant event was the 1918 Cerrillos earthquake of estimated $M_L$ 5.5, which occurred approximately 50 km southeast of LANL (Fig. 1). Despite the lack of large magnitude historical earthquakes, the geologic record indicates that many faults in the region have generated surface-faulting earthquakes (M > 6.5) during the late Quaternary.

From 1991 to 1995, the first extensive seismic hazard evaluation of LANL was performed (Wong et al., unpubl. report for LANL, 1995). State-of-the-art earthquake ground motion assessments were performed for eight LANL Technical Areas (Fig. 2). This study updates the seismic design criteria presently in use at LANL, particularly in light of the recognition that the Guaje Mountain fault, which intersects the Laboratory (Fig. 2), has been active in the Holocene (Gardner et al., 1990; Gardner and Reneau, this volume).

The specific objectives of the LANL seismic hazard evaluation were to (1) identify active faults or other potential earthquake sources in the LANL region that may significantly contribute to the seismic hazard at the Laboratory; (2) characterize the location, geometry, maximum earthquake magnitude and earthquake recurrence of these seismic sources; (3) assess the effects of the near-surface geology beneath each major facility site on strong ground shaking (>0.05 g where g is the gravitational acceleration at the earth's surface [980 cm/sec$^2$]); (4) estimate the probability of exceeding selected ground motion values by performing a probabilistic seismic hazard analysis that incorporates parametric uncertainties; (5) estimate deterministic ground motion parameters from the most significant earthquake source to compare with the probabilistic ground motion estimates using a traditional empirical approach and a state-of-the-art stochastic numerical modeling methodology; and (6) develop site-specific seismic design and seismic safety criteria for LANL. Other aspects of seismic hazards, including surface faulting and liquefaction were not addressed in this study.

## SEISMOTECTONIC SETTING

LANL is located along the western margin of the Rio Grande rift, a broad physiographic and structural depression between the Colorado Plateau on the west and the Great Plains on the east. In north-central New Mexico, it is composed of a series of north-trending, elongate topographic and structural basins that are collapsed parts of a broad area of Laramide structural uplift (Baltz, 1978). The structural basins are arranged in a right-stepping, en echelon pattern and are characterized by thin crust, high heat flow, Tertiary through late Quaternary faulting, Tertiary through Quaternary volcanism, and thick basin fills (Morgan et al., 1986). These basins exhibit evidence of east-west extension at a long-term average rate of about 0.10 to 0.14 mm/yr (Kelson and Olig, 1995). The Rio Grande rift exhibits similar geologic and geophysical characteristics to continental rifts throughout the world, such as the Kenya rift of the East African rift system and the Baikal rift of the Mongolian Plateau (Keller et al., 1991).

Seismicity in the Rio Grande rift of northern New Mexico is relatively abundant and widespread, although of small magnitude (Sanford et al., 1991). Earthquakes recorded by the LANL network from 1973 to 1992 and relocated by House and Hartse (1995) were evaluated in this study. As is commonly observed throughout the neighboring Basin and Range province, seismicity in the Rio Grande rift generally is not associated with mapped Quaternary faults or structures. Some microearthquakes in the LANL region, however, may be associated with a few mapped faults, including the Puye, La Bajada and La Cañada del Amagre-Clara Peak fault zones (Fig. 1). Only a few well-located earthquakes have occurred in the vicinity of LANL and the Pajarito fault system, including two small events of approximate $M_L$ 2 which were felt at surprisingly high intensities of Modified Mercalli (MM) VI (Gardner and House, 1994). The Valles caldera, just west of LANL, presently appears to be seismically quiescent (Fig. 1).

The maximum depth of seismicity in the northern Rio Grande rift appears to range from 12 to 15 km; the former value is consistent with slightly elevated crustal temperatures (Wong and Chapman, 1990). Based on these focal depths, a seismogenic thickness of about 15 km has been adopted for the upper crust beneath the Rio Grande rift. Focal mechanisms exhibit normal and strike-slip faulting generally on north-striking planes (House and Hartse, 1995). The modern tectonic stress field is characterized by approximate east-west extension (Zoback and Zoback, 1989).

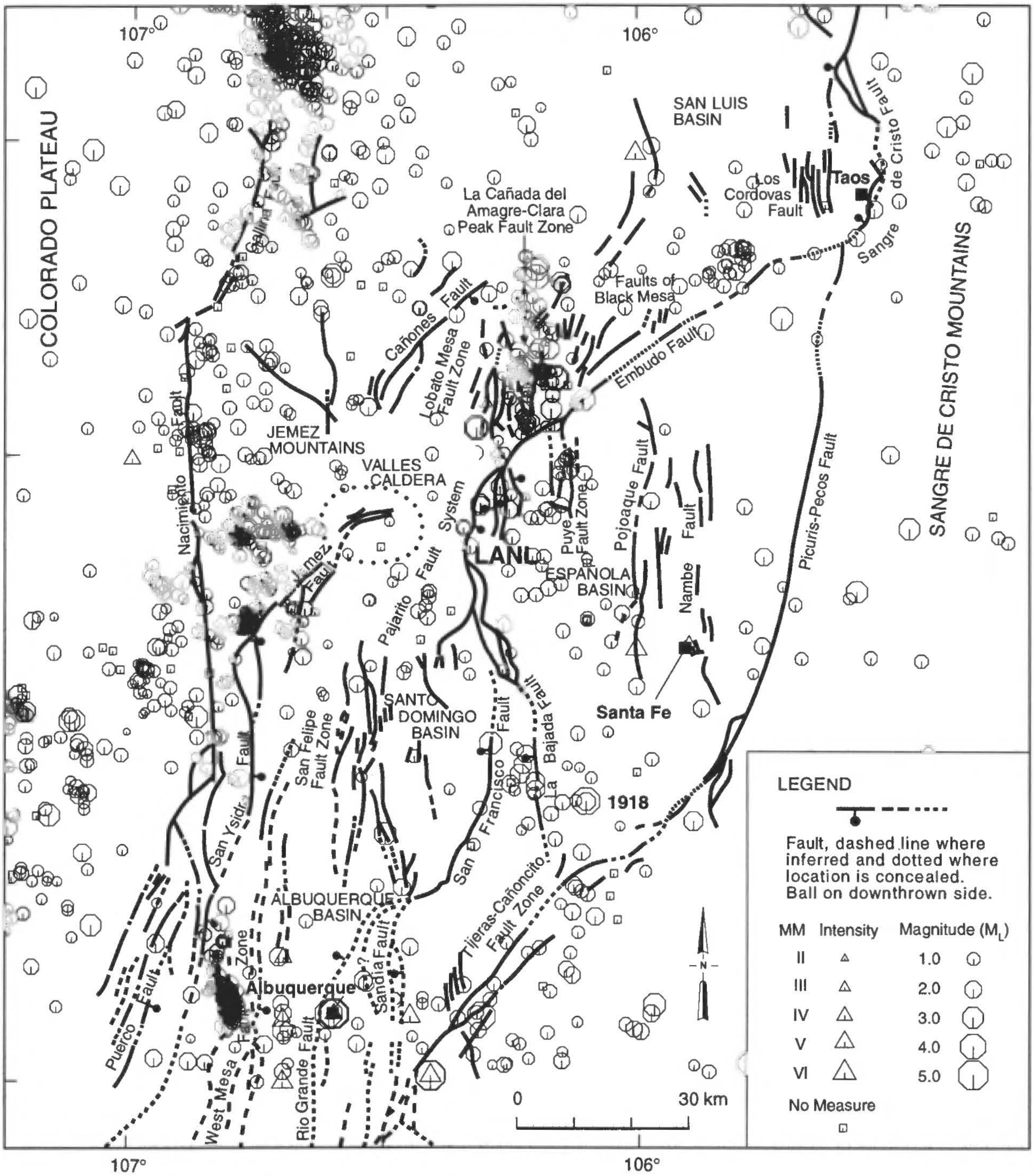


FIGURE 1. Historical seismicity (1873–1992) and active and potentially active faults in the LANL region. Seismicity and fault data from Wong et al. (unpubl. report for LANL, 1995).

## SEISMIC SOURCE CHARACTERIZATION

The probabilistic seismic hazard analysis considered both active faults and areal sources (to account for "background" seismicity not associated with known geologic structures). We identified 25 faults and four areal sources (seismic source zones) within the LANL region as potential seismic sources significant to the Laboratory in terms of ground shaking (Fig. 1; Tables 1, 2). The location, source geometry, orientation, capability or activity potential, rupture scenarios and segmentation, sense of slip, slip rate, and recurrence intervals (where available) were characterized for each fault considered in the hazard analysis using logic trees (e.g., Fig. 3). Maximum magnitudes were estimated using the empirical relationships developed by Wells and Coppersmith (1994) for rupture lengths, rupture areas, and where available, displacements (Table 1). The uncertainty incorporated into the analysis for these magnitude values is about ± 0.3 unit.

### Pajarito fault system

The three most significant and closest faults to LANL, the Pajarito, Guaje Mountain, and Rendija Canyon faults (Fig. 2), which we refer to together as the Pajarito fault system, were the primary focus of our studies. The Pajarito fault system is a 41-km-long, north-striking system of normal faults (Fig. 1) that defines the active western boundary of a portion of the Rio Grande rift (Gardner and House, 1987). The main 41-km-long Pajarito fault is located along the western margin of LANL and is a

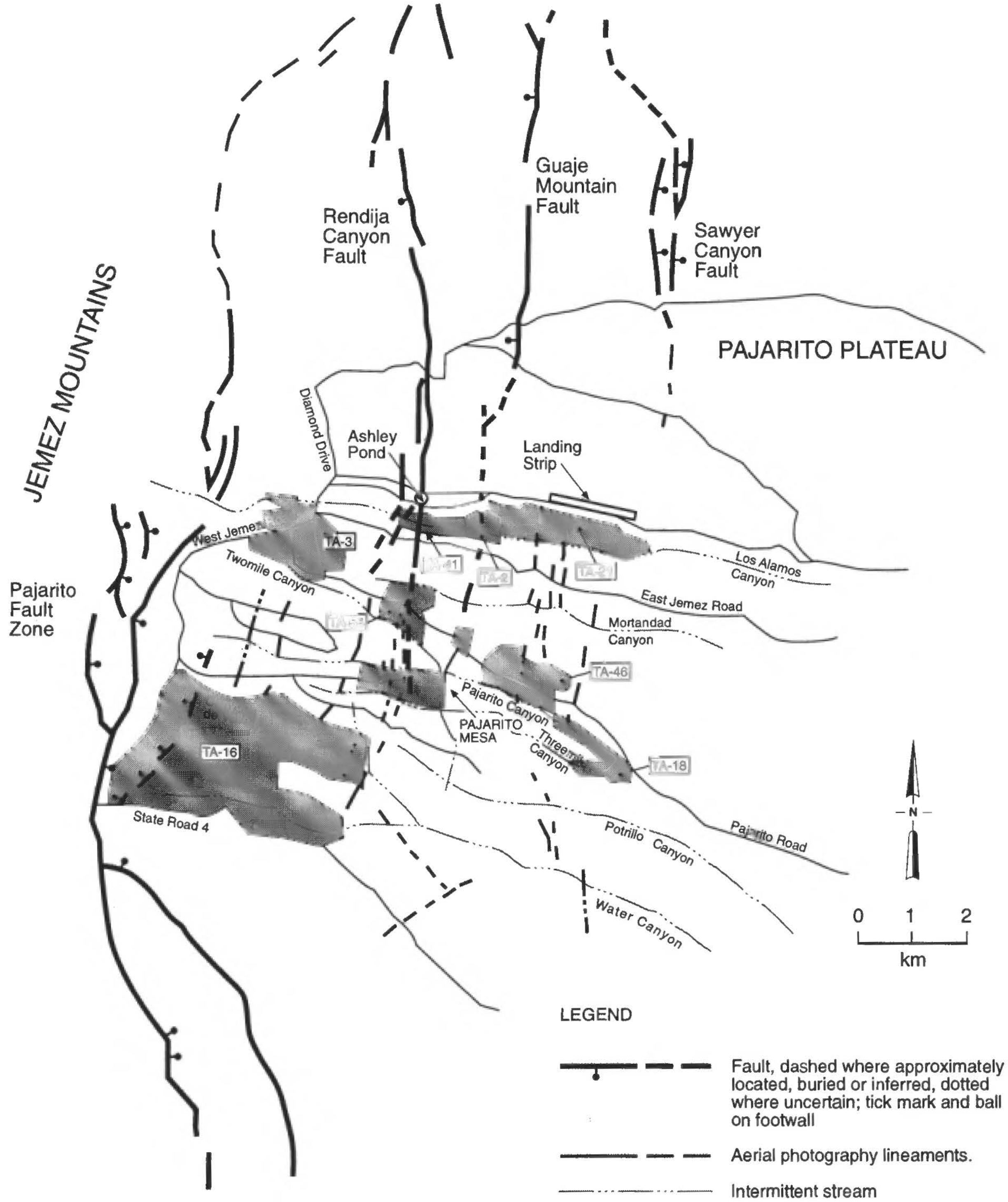


FIGURE 2. Map of LANL showing selected Technical Areas (shaded) and the Pajarito fault system.

down-to-the-east normal fault that dips beneath the Laboratory (Fig. 2). The 14-km-long Rendija Canyon fault is located 3 km east of the Pajarito fault, strikes north-south across much of LANL (Fig. 2), dips steeply to the west, and shows dominantly normal slip. The 12-km-long Guaje Mountain fault is located 1 to 2 km east of the Rendija Canyon fault (Fig. 2), and is similar to it in orientation, structural style, and sense of slip (Gardner and Reneau, this volume).

Paleoseismic investigations were conducted along the Pajarito, Rendija Canyon and Guaje Mountain faults. The results of these studies are described in detail in companion papers by Olig et al. (this volume) and Kelson et al. (this volume). Secondary faults exposed in trenches along the base of the main Pajarito fault escarpment suggest that displacement on the main fault may have occurred shortly before deposition of the El Cajete Pumice about 50 to 60 ka (Reneau et al., 1996). However, because exposures of the fault zone are incomplete, we cannot preclude the possibility of younger surface ruptures. The paleoseismic record for the main Pajarito fault remains too incomplete to determine reliable recurrence intervals. In contrast, topographic profiles along the fault provide abundant data on long-term vertical slip rates, indicating an average rate of 0.07 mm/yr for the past 1.2 Ma (Olig et al., this volume).

Evidence from trenches on the Rendija Canyon fault shows that it has ruptured repeatedly during the late Quaternary, with the most recent event

TABLE 1. Faults considered in the seismic hazard evaluation.

| Fault | Probability of Activity | Rupture Length (km) | Best Estimate Maximum Magnitude ($M_w$) | Slip Rate Best Estimate (Range) (mm/yr) | Style of Faulting |
|---|---|---|---|---|---|
| Pajarito | 1.0 | 41 | 6.9 ± 0.3 | 0.09 (0.01-0.95) | Normal |
| Rendija Canyon | 1.0 | 14 | 6.5 ± 0.3 | 0.02 (0.01-0.25) | Normal |
| Guaje Mountain | 1.0 | 12 | 6.5 ± 0.3 | 0.01 (0.01-0.14) | Normal |
| Sawyer Canyon | 1.0 | 14? | 6.5 ± 0.3 | 0.03 (0.01-0.3) | Normal |
| Puye | 1.0 | 20 | 6.3 ± 0.3 | 0.03 (0.01-0.3) | Normal |
| Lobato Mesa | 1.0 | 22 | 6.6 ± 0.3 | 0.05 (0.01-0.45) | Normal |
| La Bajada | 1.0 | 40 | 6.9 ± 0.3 | 0.07 (0.01-0.58) | Normal |
| Embudo | 1.0 | 64 | 7.0 ± 0.3 | 0.09 (0.02-0.72) | Oblique |
| Southwest Segment | 1.0 | 31 | 6.7 ± 0.3 | 0.09 (0.02-0.72) | Oblique |
| Northeast Segment | 1.0 | 30 | 6.7 ± 0.3 | 0.09 (0.02-0.72) | Oblique |
| La Cañada del Amagre/Clark Peak | 0.5 | 12 | 6.2 ± 0.3 | 0.10 (0.02-0.9) | Strike-Slip |
| San Francisco | 1.0 | 42 | 6.9 ± 0.3 | 0.07 (0.01-0.58) | Normal |
| Pojoaque | 0.5 | 49 | 7.0 ± 0.3 | 0.02 (0.01-0.23) | Normal |
| San Felipe | 0.5 | 47 | 6.8 ± 0.3 | 0.05 (0.01-0.4) | Normal |
| Santa Ana | 0.5 | 21 | 6.5 ± 0.3 | 0.05 (0.01-0.4) | Normal |
| Algodones | 0.5 | 16 | 6.4 ± 0.3 | 0.05 (0.01-0.4) | Normal |
| Jemez-San Ysidro | 1.0 | 50 | 6.9 ± 0.3 | 0.06 (0.01-0.52) | Normal |
| Jemez | 1.0 | 26 | 6.7 ± 0.3 | 0.06 (0.01-0.52) | Normal |
| San Ysidro | 1.0 | 24 | 6.6 ± 0.3 | 0.06 (0.01-0.52) | Normal |
| Cañones | 0.5 | 30 | 6.7 ± 0.3 | 0.02 (0.01-0.23) | Normal |
| Nambe | 0.1 | 50 | 7.0 ± 0.3 | 0.02 (0.01-0.23) | Normal |
| Black Mesa | 0.5 | 15 | 6.5 ± 0.3 | 0.02 (0.01-0.21) | Normal(?) |
| Tijeras Cañoncito | | | | | |
| Lamy | 0.5 | 25 | 6.6 ± 0.3 | 0.09 (0.02-0.72) | Oblique |
| San Pedro/Ortiz/Monte Largo | 0.5 | 29 | 6.7 ± 0.3 | 0.09 (0.02-0.72) | Oblique |
| Tijeras/Four Hills | 1.0 | 31 | 6.7 ± 0.3 | 0.09 (0.02-0.72) | Oblique |
| Nacimiento | 0.5 | 78 | 7.2 ± 0.3 | 0.02 (0.01-0.23) | Normal |
| Northern Segment | 0.5 | 34 | 6.8 ± 0.3 | 0.02 (0.01-0.23) | Normal |
| Southern Segment | 0.5 | 44 | 6.9 ± 0.3 | 0.02 (0.01-0.23) | Normal |
| Picuris-Pecos | 0.5 | 96 | 7.3 ± 0.3 | 0.05 (0.01-0.45) | Oblique |
| West Mesa | 1.0 | 52 | 7.0 ± 0.3 | 0.03 (0.01-0.17) | Normal |
| Puerco | 0.5 | 80 | 7.1 ± 0.3 | 0.02 (0.01-0.23) | Normal |
| Gallina | 0.5 | 40 | 6.8 ± 0.3 | 0.02 (0.01-0.23) | Normal |
| Sandia-Rio Grande | 1.0 | 45 | 6.9 ± 0.3 | 0.18 (0.03-1.91) | Normal |
| Sangre de Cristo | | | | | |
| Segments 3 + 4 | 1.0 | 32 | 6.8 ± 0.3 | 0.12 (0.06-0.29) | Normal |
| Segments 2 + 3 + 4 | 1.0 | 60 | 7.1 ± 0.3 | 0.12 (0.06-0.29) | Normal |
| Los Cordovas | 0.5 | 12 | 6.2 ± 0.3 | 0.02 (0.06-0.29) | Normal(?) |

occurring at about 9 ka or around 23 ka (Kelson et al., this volume). Estimated recurrence intervals on the Rendija Canyon fault range from 10 to 110 ka (Kelson et al., this volume), with preferred values ranging from 20 to 55 ka years (Wong et al., unpubl. report for LANL, 1995).

The Guaje Mountain fault exhibits evidence of multiple surface ruptures during the past approximately 150 to 300 ka and estimated slip rates for this period range from 0.01 to 0.03 mm/yr (Olig et al., this volume). Previous paleoseismic trenching along the Guaje Mountain fault also shows evidence for repeated late Quaternary surface faulting; the most recent event occurred about 4000 to 6000 yrs ago (Gardner et al., 1990; Gardner and Reneau, this volume).

The wide range of recurrence intervals and rates of activity for the three local faults demonstrates the considerable uncertainty that presently exists in characterizing their past earthquake behavior. Therefore, to better account for possible variations in future rates of activity, slip rates for well-studied faults in the Rio Grande rift were compiled (McCalpin, 1995). For many faults, there is more than an order of magnitude difference between long-term (125 ka or longer) and short-term (<125 ka) rates, with the latter generally being much higher. We used this distribution of slip rates to characterize uncertainties in rates for all faults whose short-term rates are poorly constrained (e.g., Pajarito fault).

Available paleoseismic information, albeit incomplete, suggests that the most recent large earthquakes on the three principal faults of the Pajarito fault system were not contemporaneous. However, because the three faults are in close proximity to each other and probably intersect at shallow depths, we considered both independent and dependent behavior for these faults (Wong et al., unpubl. report for LANL, 1995). This approach resulted in the consideration of 22 possible rupture scenarios for the Pajarito fault system. All scenarios were considered in the probabilistic analysis using logic trees. Additional paleoseismic investigations are needed to simplify this preliminary model. Based on the possible rupture scenarios, the size of the maximum earthquake expected for the Pajarito fault is $M_w$ 6.9 ± 0.3 (Table 1).

TABLE 2. Seismic source zones.

| Source Zone | Maximum Magnitude ($M_w$) | Recurrence Parameters b-value | Recurrence Parameters a-value |
|---|---|---|---|
| Rio Grande Rift | 6.3 ± 0.3 | 0.75 | -2.45 |
| Colorado Plateau Transition | 6.0 ± 0.3 | 0.90 | -2.17 |
| Southern Rocky Mountains | 6.3 ± 0.3 | 0.80 | -2.80 |
| Great Plains | 6.0 ± 0.3 | 0.70 | -2.84 |

### Regional faults

A review of available information and data provided the primary basis for characterizing the remaining 22 faults located outside the immediate LANL vicinity (Table 1). We also conducted reconnaissance studies of the nearby, potentially significant Puye and Embudo faults. For most faults, no detailed paleoseismic studies have been performed, and thus very little information is available. For these faults, comparisons with better studied faults were used to estimate their characteristics.

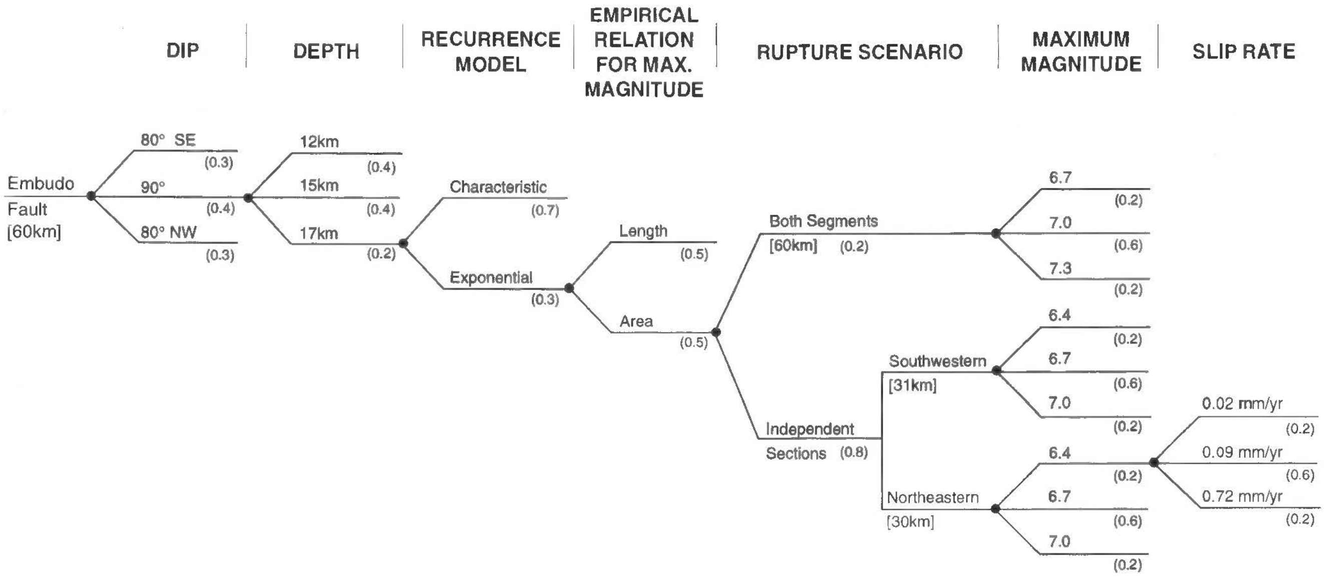


FIGURE 3. Logic tree for the Embudo fault.

Regarding fault capability or the probability of activity of the 22 regional faults, we considered all known fault zones with evidence for demonstrable Quaternary (1.6 Ma) displacement as 100% active. The probability for activity of the faults that have no evidence of Quaternary displacement or evidence of no Quaternary displacement was evaluated on a case-by-case basis. In estimating these probabilities, we considered availability and quality of data on (1) orientation and kinematic compatibility with the contemporary stress field; (2) any associated historical seismicity; (3) age and rates of most recent activity; and (4) the scale and tectonic role of the structure in accommodating extension within the Rio Grande rift. These characteristics were compiled from previous studies, analysis of aerial photography, and field reconnaissance.

All faults were modeled as single planes with the exception of the Pajarito fault system, which included multiple plane ruptures for some rupture scenarios. For faults with multiple traces at the surface that were modeled as a single plane, we assumed splays merge into one plane at a shallow depth (e.g., Puye fault zone). Rupture scenarios and dips were considered individually for each fault. To develop rupture scenarios, we used available information and criteria to delineate likely rupture segment boundaries, where appropriate. Based on the seismogenic thickness of the crust beneath the Rio Grande rift, down-dip fault widths were estimated and used to determine source-to-site distances, and in calculating rupture areas of faults that are used in estimating maximum magnitudes.

We considered both characteristic and exponential recurrence models for the faults. We characterized rates of surface faulting activity by slip rate and, where data were available, recurrence intervals based on geologic data. Slip rates are for average net slip over the fault plane. For faults that we modeled as multiple planes (e.g., certain rupture scenarios of the Pajarito fault system), we averaged slip rates for each fault plane together to properly characterize average slip for the source.

In characterizing slip rates, we found that faults in the Rio Grande rift fall into three categories: (A) faults with data on both long- and short-term slip rates; (B) faults with data only on long-term rates; and (C) faults with no available data on slip rates. We assigned values and weights for faults in category A on an individual basis according to available data. To assign values for faults in category B, we needed to account for possible differences between known long-term and unknown short-term slip rates. To do this, we compared long-term and short-term slip rates for category A faults in the Rio Grande rift. To develop a histogram of these slip rate data, McCalpin (1995) normalized the data to the long-term rate of interest. For example, for the Pajarito fault system, the data were normalized to the long-term, average vertical slip rate of 0.07 mm/yr. We then plotted a cumulative frequency distribution of the normalized slip rates and these plots were used to characterize variability from long-term rates. For faults in category C (no available slip rate data), we assumed a long-term rate similar to other analogous faults in the rift, and then assigned values and weights using the methodology for category B faults.

For all category B faults except the Pajarito fault system, we chose a three-point approximation of the slip rate distribution by assuming the long-term rate as a best estimate, weighted at 0.6, and using the 5th and 95th percentiles from the cumulative frequency plots, each weighted at 0.2 (Fig. 3). Where appropriate, we then resolved these values into dip slip values by assuming the fault dip that was given the greatest weight in the logic tree for each fault (Fig. 3).

By using slip rate data from category A faults in the Rio Grande rift to characterize uncertainty in short-term slip rates for category B faults, we assumed that temporal variations in the behavior of a particular fault can be modeled by the cumulative behavior of the better understood faults in the rift. Acquiring short-term slip rate data for category B faults is ultimately the best way to test this assumption. However, given the available data, this substitution of space for time appears to be reasonable, and it provides an internally consistent means of characterizing uncertainty in slip rates.

## Seismic source zones

Seismic source zones, or in this case, seismotectonic provinces, are defined by unique tectonic, geologic and seismologic characteristics. Provinces within the LANL region are the Rio Grande rift, the Colorado Plateau transition zone, the Great Plains, and Southern Rocky Mountains. The purpose of incorporating seismic source zones in this seismic hazard evaluation is to address the potential hazard from background earthquakes. Background earthquakes not associated with distinct tectonic features (e.g., faults or folds) were assumed to occur randomly throughout the province.

In the western U.S., the maximum magnitude for the background earthquake usually ranges between $M_L$ 6 to 6½ (Doser, 1985; dePolo, 1994). Events larger than $M_L$ 6½ are usually accompanied by surface rupture and thus repeated events of this size should produce recognizable fault or fold-related features at the earth's surface. Estimated maximum magnitudes for the background earthquakes within these four seismotectonic provinces, based principally upon the historical seismicity record, range from $M_w$ 6 to 6½ (Table 2). Recurrence for these seismic source zones was computed based upon an evaluation of the historical and contemporary seismicity (Wong et al., unpubl. report for LANL, 1995). For the Rio Grande rift in northern New Mexico, the computed recurrence parameters suggest that $M_w$ 5 and 6 earthquakes occur every 150 and 800 years, respectively. The uncertainties of these return periods are, however, extremely large and can be as much as a factor of 3 to 4.

## SITE GEOLOGY

The subsurface geology beneath LANL was investigated through a program of borehole exploration (Gardner et al., 1993), downhole velocity measurements, dynamic laboratory testing of borehole samples, and compilation and evaluation of all relevant LANL borehole and geotechnical data (Wong et al., unpubl. report for LANL, 1995). Based on site-specific geologic and shear-wave velocity profiles developed in this study, the LANL sites were grouped into two categories, mesa and canyon sites. This categorization reflects the topographic location of LANL, where most of the facilities are located on top of mesas of volcanic Bandelier Tuff (Fig. 2). A few Technical Areas are located within the adjacent canyons where the tuff is largely absent. The shear-wave profiles were used in the stochastic modeling of ground motions. Kappa, a measure of the near-surface attenuation used in the modeling, was computed by analyzing a few earthquakes recorded at LANL seismographic stations whose near-surface geology is similar to that beneath the Laboratory. A kappa value of 0.035 sec was estimated for LANL, which is typical of western U.S. rock sites (Silva and Darragh, 1995).

## DETERMINISTIC GROUND MOTION EVALUATION

Based on the above site-specific subsurface data and the seismic source characterization, deterministic and probabilistic ground motions were estimated in terms of peak horizontal accelerations and acceleration response spectra. The deterministic ground motions for the most significant earthquake to LANL, an approximate $M_w$ 7 event on the Pajarito fault, were evaluated using an empirical approach and a state-of-the-art stochastic numerical modeling methodology.

Based on the site-specific shear-wave velocity profiles, the LANL sites are most similar to deep soil sites and thus attenuation relationships developed by Joyner and Boore (1988), Campbell and Bozorgnia (1994), and Sadigh et al. (described in Joyner and Boore [1988]), which are appropriate for such site conditions, were used in the empirical analysis. The relationships yielded average peak horizontal accelerations of 0.47 to 0.53 g at the eight Technical Areas for the $M_w$ 7 Pajarito fault event at source-to-site distances of about 0.5 to 6 km.

Site-specific stochastic acceleration response spectra were computed based upon the Band-Limited-White-Noise source model and random vibration theory (Silva et al., 1990). The stochastic peak horizontal accelerations (0.60 to 0.62 g) computed for a $M_w$ 7 Pajarito fault earthquake at the mesa sites were slightly higher than the empirically calculated values. In contrast, high-frequency site amplification due to the strong velocity contrasts in the volcanic stratigraphy occurs at the three canyon sites, with peak horizontal accelerations ranging from 0.8 to 0.9 g. These values significantly exceed the empirical values. The offsetting effects of amplification and damping of the seismic waves in the Bandelier Tuff probably account for the low peak accelerations at the mesa sites. The differences between the peak accelerations from the empirical analysis and modeling are not unexpected given the unique subsurface geology beneath the LANL and possible source effects that are not generally accounted for in empirical attenuation relationships (Wong and Silva, 1994).

In addition to the effects of site geology, the possible effects of the mesa topography on ground motions were analyzed using a numerical finite-difference modeling technique (Wong et al., unpubl. report for LANL, 1995). Based upon this first-order analysis, topographic amplification of 10 to 20% in the period range of 0.2 to 1.0 sec is likely to occur at LANL mesa top sites.

## PROBABILISTIC SEISMIC HAZARD ANALYSIS

Seismic hazard curves for peak horizontal acceleration and response spectral accelerations at periods of 0.2 and 1.0 sec were developed for the eight selected LANL Technical Areas. These curves were computed based upon a probabilistic seismic hazard analysis (e.g., Cornell, 1968) using a logic tree approach. This approach allows for incorporation of the full range of possible source, path, and site parameters and their uncertainties (Fig. 3). The 25 faults and four seismic source zones were modeled in the analysis. Ground motion attenuation was characterized through the use of site-specific relationships developed for each Technical Area based on stochastic numerical modeling (Wong et al., unpubl. report for LANL, 1995) and the same empirical relationships used in the deterministic ground motion analysis.

Seismic hazard curves for peak horizontal acceleration and for a typical site at LANL are shown in Figure 4, and ranges of mean peak horizontal accelerations for the LANL Technical Areas for the four return periods required by the DOE are shown in Table 3. For the 500-year return period, which corresponds to a value typically used in standard building codes (such as the Uniform Building Code), the peak horizontal acceleration is 0.14 to 0.15 g. For comparison, soil sites in the Salt Lake City area adjacent to the seismically active Wasatch fault have 500-year return period peak horizontal accelerations of about 0.25 to 0.30 g (Wong et al., 1995b). For a return period of 10,000 yrs, which might be appropriate for critical structures, the LANL peak accelerations are significant at 0.53 to 0.57 g (Table 3).

The most significant seismic source contributing to the peak acceleration hazard at the LANL is the Pajarito fault system and, to a lesser degree, the Rio Grande rift source zone (Fig. 5). Because all the evaluated Technical Areas at LANL are at about the same distance from the Pajarito fault system, the variability in peak horizontal accelerations from site to site is small (Table 3). Seismic sources that are minor contributors to the ground shaking hazard at LANL include the Embudo, Puye, Lobato Mesa, Sawyer Canyon and La Bajada faults (Fig. 5).

Based on the results of the probabilistic seismic hazard analysis, uniform hazard spectra for the four DOE return periods were calculated (Wong et al., unpubl. report for LANL, 1995). Design spectra were then developed and synthetic time histories generated for use in seismic design and seismic safety analyses of Laboratory facilities.

## CONCLUSIONS

We recently completed a state-of-the-art seismic hazard evaluation of LANL, which is located along the western margin of the Rio Grande rift

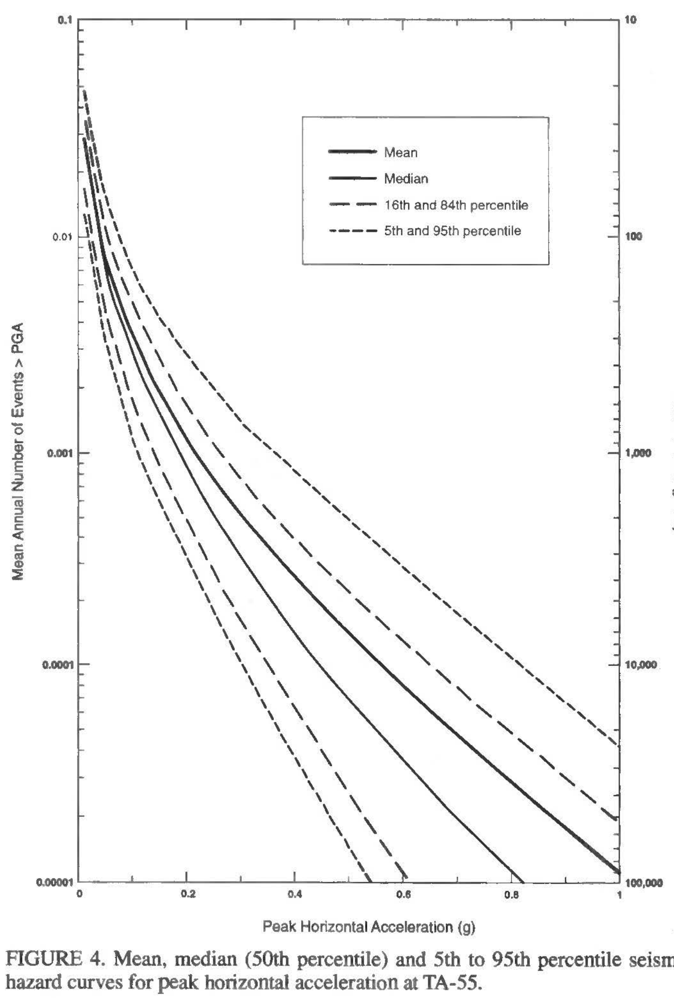


FIGURE 4. Mean, median (50th percentile) and 5th to 95th percentile seismic hazard curves for peak horizontal acceleration at TA-55.

TABLE 3. Site-specific probabilistic peak horizontal accelerations.

| Return Period | Peak Horizontal Acceleration (g's) |
|---|---|
| 500 yrs | 0.14 - 0.15 |
| 1,000 yrs | 0.21 - 0.22 |
| 2,000 yrs | 0.29 - 0.31 |
| 10,000 yrs | 0.53 - 0.57 |

in northern New Mexico. The potential contributions to the ground shaking hazard at LANL from 25 active and potentially active faults, and the background seismicity in four areal seismic source zones, were integrated through a probabilistic seismic hazard analysis. Although few fault-specific studies have been performed in the Rio Grande rift in northern New Mexico, the range of fault parameters and their uncertainties for the 25 faults were incorporated into the probabilistic analysis. (Even for those faults which have been studied, uncertainties can be large, e.g., Pajarito fault.) The effects on ground motions from crustal attenuation and the near-surface geology specific to the Rio Grande rift and the LANL area, respectively, were also incorporated into the estimates of ground motions. The results of the probabilistic seismic hazard analysis indicate that the ground shaking hazard at the LANL is higher than might be indicated by the historical record and therefore higher than is commonly believed possible. Ground motion levels are comparable to some areas along the Intermountain seismic belt in central Utah and in the Basin and Range province of southern Nevada (Wong et al., 1995a).

## ACKNOWLEDGMENTS

This study was performed by the personnel of Woodward-Clyde Federal Services (WCFS); its subcontractors, William Lettis & Associates (WLA) and Pacific Engineering & Analysis (PE&A), and members of the Earth and Environmental Sciences Division of LANL. Many individuals in addition to the authors contributed to this study and to them we would like to express our sincere gratitude: Janet Sawyer, Andy Gorton, Doug Wright, Clark Fenton, Sue Penn and Norma Biggar of WCFS; Tom Sawyer formerly of WCFS; Helen Kanakari, Susan Chang, Sadako McInerney, Fumiko Goss, Anita Quintana, Said Salah-Mars, Jim Springer and Perry Jung of Woodward-Clyde Consultants; Colleen Haraden, Jeff Unruh, Gary Simpson, Jay Noller and Bill Lettis of WLA; Cathy Stark, Sylvia Li and Ky Lang of PE&A; Leigh House, Suzanne Meuret, John Carney, James Lakings, Larry Goen, Scott Baldridge and Karen Carter of LANL; Bruce Redpath of Redpath Geophysics; Ken Stokoe of the University of Texas; Steve Forman of The Ohio State University; and Jim McCalpin of GEO-HAZ Consultants. Special gratitude to Dean Keller, Doug Volkman and Jeff Kimball for their support of our efforts. Technical reviews of various aspects of this study were provided by Mike Machette, USGS; James

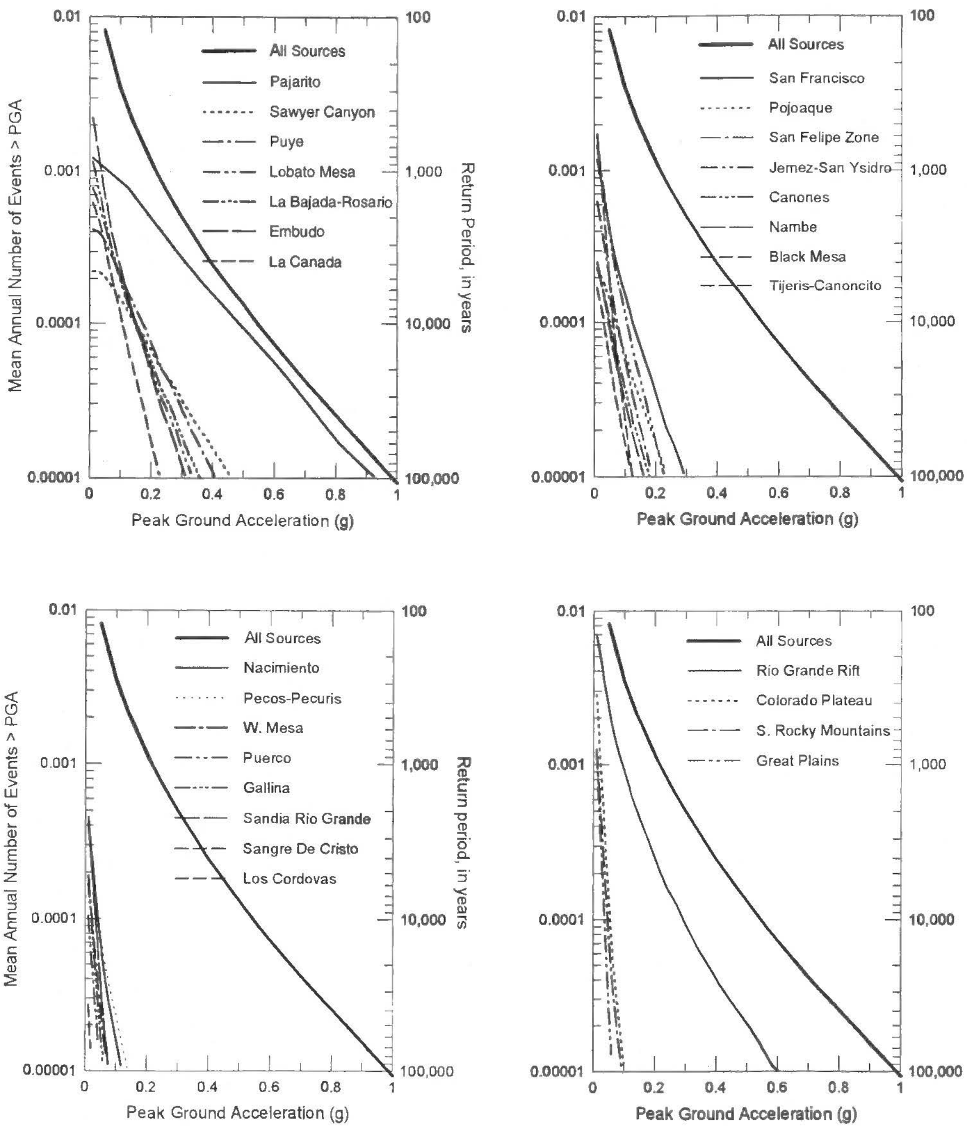


FIGURE 5. Contributions of seismic sources to the mean seismic hazard in terms of peak horizontal acceleration at TA-55.

McCalpin; Al Sanford, New Mexico Tech; Mike Cline, WCFS; Bob Youngs, Geomatrix Consultants; Jeff Kimball, DOE; Bill Lettis; and Carl Costantino, City College of New York. Reviews of this paper by Clark Fenton and Andy Gorton of WCFS are appreciated. These studies were supported by LANL Contracts 9-XT1-092K-1 and 5175F0013-9Y.

## REFERENCES

Baltz, E. H., 1978, Resume of Rio Grande depression in north-central New Mexico: New Mexico Bureau of Mines and Mineral Resources, Circular 163, p. 210–228.

Campbell, K. W. and Bozorgnia, Y., 1994, Near-source attenuation of peak horizontal acceleration from worldwide accelerograms recorded from 1957 to 1993: Fifth U.S. International Conference on Earthquake Engineering, v. 3, p. 283–292.

Cornell, C. A., 1968, Engineering seismic risk analysis: Bulletin of the Seismological Society of America, v. 58, p. 1583–1606.

dePolo, C. M., 1994, The maximum background earthquake for the Basin and Range Province, western North America: Bulletin of the Seismological Society of America, v. 84, p. 466–472.

Doser, D.I., 1985, The 1983 Borah Peak, Idaho and 1959 Hebgen Lake, Montana earthquakes—models for normal fault earthquakes in the Intermountain seismic belt; *in* Stein, R. S. and Bucknam, R. C. (eds.): Proceedings of Workshop XXVIII on the Borah Peak, Idaho, Earthquake, U.S. Geological Survey, Open-File Report 85-290, p. 368–384.

Gardner, J. N., Baldridge, W. S., Gribble, R., Manley, K., Tanaka, K., Geissman, J. W., Gonzalez, M. and Baron, G., 1990, Results from seismic hazards trench #1 (SHT-1), Los Alamos seismic hazards investigations: Los Alamos National Laboratory Report EES1-SH90-19, 57 p.

Gardner, J. N. and House, L., 1987, Seismic hazards investigations at Los Alamos National Laboratory, 1984-1985, Los Alamos National Laboratory Report LA-11072-MS, 76 p. + maps.

Gardner, J. N. and House, L., 1994, Surprisingly high intensities from two small earthquakes, northern Rio Grande rift, New Mexico: EOS, Transactions, American Geophysical Union, v. 75, p. 240.

Gardner, J. N., Kolbe, T. and Chang, S. 1993, Geology, drilling, and some hydrologic aspects of seismic hazards program core holes, Los Alamos National Laboratory, New Mexico: Los Alamos National Laboratory Miscellaneous Report, LA-12460-MS.

Gardner, J. N. and Reneau, S. L., 1996, Holocene faulting and sedimentation within the Guaje Mountain fault zone: New Mexico Geological Society, Guidebook 47.

House, L. and Hartse, H., 1995, Seismicity and faults in northern New Mexico: New Mexico Geological Society, Guidebook 46, p. 135–137.

Joyner, W. B. and Boore, D. M., 1988, Measurement, characterization and prediction of strong ground motion; *in* Von Thun, J. L. (ed.): Proceedings of the conference on earthquake engineering and soil dynamics: Recent Advances in Ground Motion Evaluation, American Society of Civil Engineers, p. 43–103.

Keller, G. R., Khan, M. A., Morgan, P., Wendlandt, R. F., Baldridge, W. S., Olsen, K. H., Prodehl, C. and Braile, L. W., 1991, A comparative study of the Rio Grande and Kenya rifts: Tectonophysics, v. 197, p. 355–371.

Kelson, K. I., Forman, S. L., Gardner, J. N., Hemphill-Haley, M. A., Kolbe, T. K., Olig, S. S., Reneau, S. L., Simpson, G. D. and Wong, I. G., 1996, Latest Pleistocene and possibly Holocene displacement along the Rendija Canyon fault, Los Alamos County, New Mexico: New Mexico Geological Society, Guidebook 47.

Kelson, K. I. and Olig, S. S., 1995, Estimated rates of Quaternary crustal extension in the Rio Grande rift, northern New Mexico: New Mexico Geological Society, Guidebook 46, p. 9–12.

McCalpin, J. P., 1995, Frequency distribution of slip rates for normal faults in the western USA: Bulletin of the Seismological Society of America, v. 85, p. 1867–1872.

Morgan, P., Seager, W. R. and Golombek, M. P., 1986, Cenozoic thermal, mechanical and tectonic evolution of the Rio Grande rift: Journal of Geophysical Research, v. 91, p. 6263–6276.

Olig, S. S., Kelson, K. I., Gardner, J. N. and Reneau, S. L., 1996, The earthquake potential of the Pajarito fault: New Mexico Geological Society, Guidebook 47.

Reneau, S. L., Gardner, J. N. and Forman, S. L., 1996, New evidence for the age of the youngest eruptions in the Valles caldera, New Mexico: Geology, v. 24, p. 7–10.

Sanford, A. R., Jaksha, L. H. and Cash, D. J., 1991, Seismicity of the Rio Grande rift in New Mexico: *in* Slemmons, D. B., Engdahl, E. R., Zoback, M. D., and Blackwell, D. D. (eds.), Neotectonics of North America: Geological Society of America Decade Map, v. 1, p. 229–244.

Silva, W. J. and Darragh, R. B., 1995, Engineering characterization of strong ground motion recorded at rock sites: Electric Power Research Institute, EPRI TR-102262.

Silva, W., Darragh, R., Stark, C., Wong, I., Stepp, J. C., Schneider, J. F. and Chiou, S., 1990, A methodology to estimate design response spectra in the near-source region of large earthquakes using the Band-Limited-White-Noise ground motion model: Proceedings, Fourth U.S. National Conference on Earthquake Engineering, v. 1, p. 487–494.

Wells, D. L. and Coppersmith, K. J., 1994, New empirical relationships among magnitude, rupture length, rupture width, rupture area, and surface displacement: Bulletin of the Seismological Society of America, v. 84, p. 974–1002.

Wong, I. G. and Chapman, D. S., 1990, Deep intraplate earthquakes in the western U.S. and their relationship to lithospheric temperatures: Bulletin of the Seismological Society of America, v. 80, p. 589–599.

Wong, I. G., Green, R. K., Olig, S. S. and Youngs, R. R., 1995a, Assessing seismic hazards in regions of large infrequent earthquakes: examples from the Basin and Range province: International Union of Geodesy and Geophysics XXI General Assembly, Abstracts Week B, p. B356.

Wong, I., Olig, S., Green, R., Moriwaki, Y., Abrahamson, N., Baures, D., Silva, W., Somerville, P., Davidson, D., Pilz, J. and Dunne, B., 1995b, Seismic hazard evaluation of the Magna tailings impoundment; *in* Lund, W. R. (ed.), Environmental and engineering geology of the Wasatch Front region: Utah Geological Association Publication 24, p. 95–110.

Wong, I. G. and Silva, W. J., 1994, Near-field ground motions on soil sites: augmenting the empirical database through stochastic modeling: Proceedings, Fifth U.S. National Conference on Earthquake Engineering, v. 3, p. 55–65.

Zoback, M. L. and Zoback, M. D., 1989, Tectonic stress field of the continental United States: Geological Society of America, Memoir 172, p. 523–540.